



A MANFIS-based geometric deviation prediction and optimal parameter selection for SPIF geometric accuracy improvement

D. Moses Raja Cecil¹

Accepted: 9 September 2021 / Published online: 4 October 2021

© The Author(s), under exclusive licence to Springer-Verlag GmbH Germany, part of Springer Nature 2021

Abstract

In the manufacturing sector, the section that has attained the most demand is metal forming. Most traditional methods in the manufacturing industry are not flexible, thus opted for the single point incremental forming (SPIF) method. However, it encompasses a geometric deviation issue. The prediction of geometric deviation and optimal parameter selection is more tedious in the existing works. In order to trounce these issues, this paper proposes a modified adaptive neuro-fuzzy inferences system (MANFIS)-centred geometric deviation prediction and enhanced squirrel search algorithm (ESSA)-centred optimal parameter selection for SPIF in AA2024-O aluminium alloy sheets. The proposed methodology encompasses '3' sections. Initially, the SPIF designing is performed in which truncated cone shape is chosen and inputted into Computer-Aided Designs/Computer-Aided Manufacturing software. Next, the designed shape is constructed and coordinate-measuring machines gauges the geometric metrics. Therefore, to envisage the geometric deviations, the measured geometric values are rendered as the input to the MANFIS. If the deviation is presented, then the ESSA algorithm chooses the optimal initial parameters, and that selected parameters are suggested to the SPIF design. The minimum roundness deviation together with the position deviation is fixed as the Fitness Function in ESSA. The AA2024-O aluminium alloy sheet is taken for the experimental investigation. In addition, the proposed method's performance is contrasted with prevailing methods centred on statistical metrics and MSE, which exhibits that the proposed methods outweigh the prevailing methods. A better result is attained by the proposed works when analogized to the existent methods by obtaining values of 97.90%, 96.78%, 95.84%, 96.23%, and 0.017% for accuracy, precision, recall, F-measure along with mean error.

Keywords Modified adaptive neuro-fuzzy inference system (MANFIS) · Enhanced squirrel search algorithm (ESSA) · Roundness deviation · Position deviation · AA2024-O aluminium alloy sheet

Abbreviations

SPIF	Single point incremental forming	GA	Genetics algorithm
MANFIS	Modified adaptive neuro-fuzzy inferences system	BPNNs	Backpropagation neural networks
CAD/	Computer-aided designs/computer-aided	GBRT	Gradient boosting regression tree
CAM	manufacturing	Al/SUS	Aluminium or stainless steel
CMM	Coordinate measuring machines	RSM	Response surface methodology
FF	Fitness function	CV	Cross-validation
ESSA	Enhanced squirrel search algorithm	NN	Neural networks
GE	Geometric error	ANFIS	Adaptive neuro-fuzzy inferences system
ANN	Artificial neural networks	MF	Membership functions
MSE	Mean squared errors	SSA	Squirrel search algorithms
FEA	Finite elements analysis	HT	Hickory tree
		CNN	Convolutional neural network
		SVR	Support vectors regressions
		PSO	Particle swarms optimization

✉ D. Moses Raja Cecil
mosesrajaphd@yahoo.com

¹ Department of Mechanical Engineering, Loyola ICAM
College of Engineering and Technology, Chennai, India

1 Introduction

The major component of the contemporary manufacturing industry is metal forming (Panjwani et al. 2017). On account of the large competition in the market, the demand aimed at minimized manufacturing time along with costs has brought forth the commencement of new technologies and processes. Various advanced forming technologies, like SPIF, that is the kind of incremental sheet forming (ISF) techniques have come out to tackle the requirement for flexible and small production batches (Azevedo et al. 2015). The SPIF is basically a extremely flexible process that utilizes a single generic tool for an unlimited variety of shapes with huge potential for the generation of new or replacement parts that are short lived (Li et al. 2015a). Recently, owing to the decrease in the product life cycle, high demand, and customization, flexibility in sheet metal forming (SMF) has received attention (Li et al. 2014). The ISF is disparate from the traditional SMF process like pressing, drawing, stamping process, etc. Centred on the localized deformation's characteristics and the mechanism of the fracture or damage behaviours (Said et al. 2017), ISF has top-level advantages, namely low cost with simple along with economical tooling configuration and a short leading time (Dai et al. 2019). Moreover, the time, economic cost for fabrication, storage, along with maintenance of the dies/punches are fairly high in the traditional SMF techniques (Amino et al. 2014; Cao et al. 2012).

One among the important features of the metal forming industries is the geometric accuracy of the last parts. Nevertheless, the ISF technique's key drawback is bad geometric accuracy (Lu et al. 2015; Li et al. 2015b). The lack of tooling causes the raise in geometric deviations from the design shape that deters the prevalent industrialization start-up process (Khan et al. 2014). Sheet spring back causes the geometric error (GE) between the target and the formed shape (Fu et al. 2012). The major issues in every sheet manufacturing technology are the spring back which indicates the changed shape of the formed part when the tool is free or the part is unclamped (Zhang et al. 2016). Moreover, the vital factor that causes the GE is the position deviation and roundness deviation (Dabwan et al. 2020), and also pillow effect is another factor that increases the GE (Alinaghian and Honarpisheh 2019). SPIF parts with low wall angle geometry characteristically give a constructed geometry, which efficiently varies from the model surface, caused by the unnecessary bulging deformation. The development of bulge on the base part may result in the sheet wrinkles at the bulged area that causes high generating forces and also could even end the forming procedure (Mohammadi et al. 2014). To trounce the geometric inaccuracy problems, various researches in SPIF

have been performed over the last some decennium (Fischer et al. 2019), along with that various strategies were executed to conquer such issues (Kumar and Belokar 2019).

To examine the prediction, optimization, and formability of parameters in SPIF of disparate sheet metals by various approaches, namely soft computing, numerical, and analytical techniques, the research work is conducted (Maji and Kumar 2019). Few prevailing research methods directly choose the optimal parameter, and later, design the chosen shape. However, when the chosen shape is already precise, the parameters were not needed mostly. Whilst designing the selected shape, selecting the parameters by optimization method draws maximum time. Earlier prediction and then selecting the optimal parameters draws minimum time and ameliorates geometric accuracy. Thus, the paper proposed a MANFIS-centred geometric deviation and selection of optimal parameters by ESSA for SPIF in the material of aluminium.

The contribution of the presented work is proffered as follows:

- The issues of geometric prediction are easily solved by a MANFIS which is proposed with the utilization of the triangular membership functions when contrasted to the bell membership function.
- Utilizing the enhanced squirrel search algorithm (ESSA), the optimal input parameters, namely tool path, tool diameter, sheet thickness, tool shape, wall angle, step size, along with spindle speed are chosen.

The paper's structure is given as follows:

The contemporary artworks linked with the geometric deviation prediction and optimal parameters selection and their shortcomings are elucidated in the second section. The designing of the SPIF, MANFIS-based deviation prediction, and the optimal parameter selection by the usage of ESSA algorithm is given in the third section. The proposed technique's performance is analogized with the existent method in the fourth section. Lastly, the fifth section deduces the proposed work and also elucidates future improvement.

2 Literature survey

Amrut Mulay et al. (2019) formed a prediction design to calculate the maximal forming angle and average surface roughness centred upon artificial neural networks (ANN) whilst forming SPIF in AA5052-H32 substances. To construct the ANN, a feed-forward backpropagation network utilizing the Levenberg–Marquardt was created. To substantiate the concurrence among the ANN experimentation and envisage outcomes, the confirmation runs were

executed. The ANN was efficient in envisaging the process response with good precision and brought about a mean absolute percentage error, mean squared errors (MSE), and R-value of 5.96, 0.0209, together with 0.99807% for mean surface roughness; whereas for the maximal forming angle, it was 0.003, 0.0281, 0.99913, respectively. ANN algorithm was utilized by this framework. Usually, the ANN had random weight updation that took further time to implement the process.

Isidore et al. (2016) concentrated on finite elements analysis (FEA) to envisage along with control pillowing by changing the tool shape and size in SPIF. Since the tool-ends geometry altered to flat as of spherical, the in-plane stresses on the transverse directions changed its nature to tensile from compressive. Moreover, as the equipment radius augmented, the magnitude of suitable in-plane stresses reduced. It was determined that both the flat end tool and large radius delayed the pillow formation centred on the measurement as of FEA design. Nevertheless, it was discovered that the impact of differing end tool shapes from hemispherical to the flat was more vital than the differing tool radius as in the transversal direction since the deformation zones persisted in tension when forming by end flat tools. Thickness, size, and angle parameters were not pondered by the study, and thus, the geometric deviation was not wholly estimated.

Sbayti et al. (2019) proffered an enhancement scheme aimed at the geometric accuracy, centred on the recent grasshopper optimization, genetics algorithm (GA) together with global optimum determination by employing the linking together with interchanging kindred evaluator solver (GODLIKE) algorithm. It was verified and examined. The possibility to attain the sound components having fewer geometric errors, namely bending, pillow effect, and spring back errors using an appropriate selection of optimal parameters was showed by concurrently manufactured and simulated denture plate parts. The reduction of defects in shape among the target design and the attained geometry by CAD was completed by coupling the numerical simulation, and improvement methods were exhibited by the results. This method utilized the usual grasshopper algorithm that had a downside of convergence rates. Thus, the system goes via the convergence rate issue.

Taherkhani et al. (2018) aimed to choose the appropriate forming parameters to make metal sheet parts, which encompassed dimensional precision and enhanced surface quality in a short period. Sheet thickness, tool diameter, feed rate together with tool step depth were the '4' parameters chosen as design variables. These parameters were wielded for the process design using the group technique of data handling ANN. Using SPIF experimentation executed on the computers numerical control milling machine through central composite design, the necessary

data for creating the empirical designs were attained. The design variables of a trade-off point in the experimental study were examined, and thus, the analysis showed the model's efficiency and precision. It may give bad outcomes because this method had not resolved the issue of weight value selection in ANN.

Sbayti et al. (2017) proffered enhancement features of SPIF parameters aimed at titanium denture plates. The numerical simulation centred on the Box–Behnken experimental design along with the response surface methods determined the enhancement strategy. The application to discover the optimal result was offered by the multiple-objective genetic algorithm together with the GODLIKE algorithm. Maximum forming force, reducing the sheet thickness along with the final attained depth, was pondered as objectives. The denture plate was built by SPIF with optimum parameters for results assessment. Centred on the system of optical measurement, the analogy of final geometry with the target geometry had been performed. It was exhibited that the implemented techniques gave a robust method aimed at the optimum parameters selection in SPIF. Straightly applied optimization algorithm took added time to do the process.

Hartmann et al. (2016) suggested an ANN for the production of tool paths in ISF. Proper network output and input structure were designed for the ISF. For suitable training, balanced sample data sets were created. The impact of several training algorithms, training sets, and network configurations was studied related to a feed-forwards network structure by backpropagation. At last, by employing the production of automated sheet part, the computer incorporated manufacturing method was subjected to verification. This method had stability issues, which happened on account of the architecture structure unless the ANN was not capable of generalizing as of the training set.

Liu and Li (2019) propounded a virtual data generation approach centred on megatrend diffusion function along with particle swarm optimization algorithm for improving the SPIF force prediction's accuracy given in small experimental data problems. Utilizing a small amount of force data attained as of pyramidal shape forming, the proposed modelling method was confirmed. It was established that by including the produced virtual data in real experimental small datasets, the established prediction model's accuracy could be enhanced that proffered a good predictive capability in designing the forming force of SPIF under disparate process circumstances. The proposed model's performance with the augment in the size of the training dataset was affected by the Slowness and the unreliable nature of the feed-forward backpropagation neural networks (BPNNs).

Ali et al. (2019) introduced a study in which gradient boosting regression tree (GBRT) was utilized for determining the relationship between operating parameters and the formability along with the quality of aluminium or stainless steel (Al/SUS) bimetal sheets in different layer configurations. For creating a precise and quick prediction model, the GBRT was used, which was a machine learning technique. The D-Optimal design centred on response surface methodology (RSM) was utilized for establishing the training dataset owing to the design's good qualities, which fit the present work's criteria. For implementing this design that comprised a truncated pyramidal component with changeable wall angles, the SPIF technique was employed. After that, for tuning the GBRT's parameters, the grid search cross-validation (CV) approach was applied. Lastly, centred on disparate operating parameters along with layer arrangements of truncated pyramid parts, the microstructure observation for the contact and non-contact surfaces was examined. After a specific level, the augment in the number of trees did not augment the model's performance because of the way of construction of GBRT.

It could be recognized from the above addressed preceding works that the previous work has several limitations. The issue of random weight updation along with generalization error affected the neural network approaches whilst optimization algorithms implied in the existent works suffered from the convergence problem along with longer execution time. Apart from these limitations, due to the non-consideration of significant parameters, numerous methods were not capable of producing good results. For solving these issues, a MANFIS-centred geometric deviation prediction along with optimal parameter selection for SPIF is proposed in the subsequent section.

3 Proposed geometric deviation prediction and optimal parameter selection for SPIF in aluminium material

Propitious flexible manufacturing technology in the production of sheet elements in smaller batches without any requirement for exorbitant dies or tools is the ISF. In the last decennium, several studies were performed based on disparate strategies to ameliorate the geometric accuracy, but the crucial issue of ISF is the low geometric accuracy which considerably restricts the industrial application of this flexible forming technology as a result of the issues namely weight updation in numerous machine learning techniques. For enhancing the geometric accuracy, researches were performed by the prevailing research methods. However, optimal parameters were directly chosen by the methods. Owing to the premature convergence along with

the trapping of solution into local minima, this sort of process requires more time. That is the chief reason that this paper proposed MANFIS-centred geometric deviation prediction as well as optimal parameter selection by utilizing the ESSA in SPIF. The proposed work encompasses '3' steps: (i) SPIF design, (ii) deviation prediction, and (iii) optimal parameter selection. First, the design is performed by means of the CAD/CAM software. And then, it is designed in the milling machine. After manufacturing, the CMM gauges the deviation factors. Secondly, to ensure whether the gauged values have deviated or not, the deviation factors are inputted to the MANFIS. The optimal input parameters, namely tool path, tool diameter, sheet thickness, tool shape, wall angle, step size, along with spindle speed, are chosen by employing the proposed ESSA if the deviation took place in the third step. And that selected parameter is suggested to the SPIF design for additional manufacturing (i.e. mainly suggested to CAM). If it has not deviated, there is not any need for choosing the optimal parameters. Selecting and utilizing this technique in-turn makes the system quicker and lessens the GE. The proposed study's design is exhibited in Fig. 1.

3.1 SPIF design

The SPIF designing method is explicated in this initial stage. The geometric accuracy of a part attained using SPIF rely on various factors, namely the spring back, deformation mechanism as well as residual stresses. Five phases were followed to perform a test sequence in SPIF relying on the state and experimental arrangement and the intricacy of the process. At first, the design's shape is selected. Here, the truncated cone is selected as standard geometry and SPIF experiments were done on the AA2024-O aluminium alloy sheets that find applications in the automobile as well as aerospace industries. 250 mm × 250 mm is the sheet's size. The shape is produced with various wall angles, namely 60°, 65°, and 70°. Next, the model is done on the CAD software. After that, the program is run by the CAM tool in the machining phase. Once the simulation process is over, controlling and designing are transferred to the real-time manufacturing machine, and the machine was equipped with a steel tool. Grounded on the designed shape by the CAD, the inputted parameters were formed by the CAM. The sheet thickness, tool path, spindle speed on the forming depth, wall angle, tool diameter, tool shape as well as step size are the input parameters. After completing the construction, the control of the parts was obtained utilizing the CMM tool, i.e. the geometric associated metric, namely position and roundness were determined. Centred on these metrics, the spring back together with the pillow effects were attained; thus, these metrics are significant.

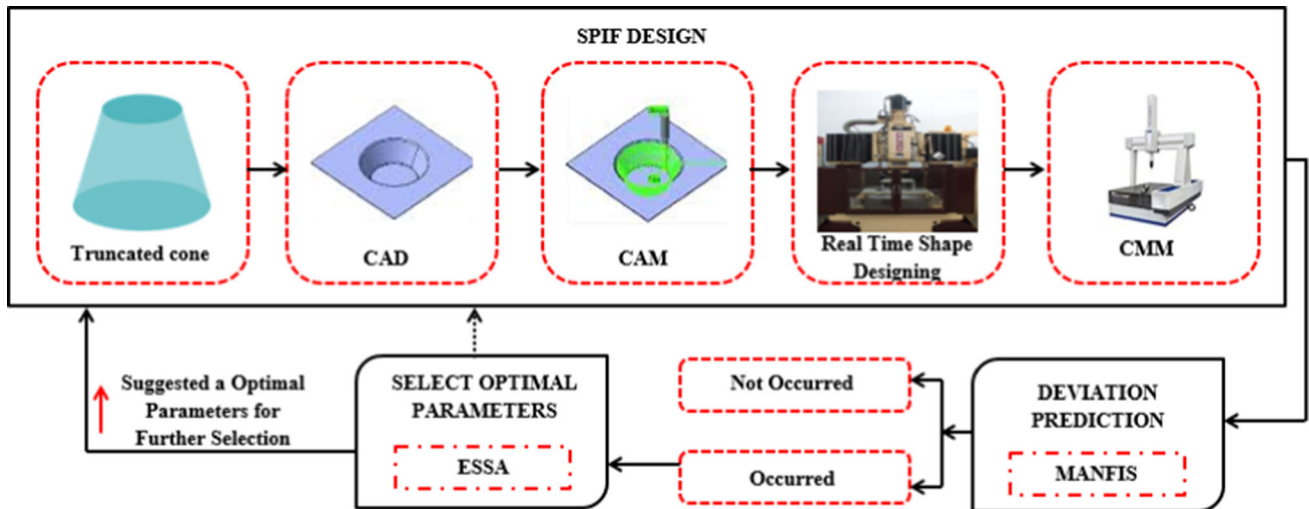


Fig. 1 Design of the presented study

3.2 Deviation prediction

The input given to the MANFIS is the geometric metrics that are attained, namely roundness measurement τ_1 , position measurements τ_2 . Alteration of the conventional neural networks (NN) by integrating it with fuzzy logic is termed the adaptive neuro-fuzzy inferences system (ANFIS) (Ibrahim et al. 2015). Takagi–Sugeno fuzzy system, which is the commonest sort of fuzzy inference systems, can well be integrated into an adaptive network. A linear relationship is its output. Assessment of its parameters can well be performed utilizing the amalgamation of gradient descent-centred error backpropagation together with the least squared error method. The network contains 2 parts: (i) antecedent, which is the first part, and (ii) conclusion part which is connected by rules on the network form is the second part. The ANFIS encompasses '5' layers. A fuzzification process is performed by the first layer; the fuzzy AND operation of the antecedent of the fuzzy rules are executed in the second layer, the membership functions (MF) is normalized by the third layer, the resultant part of the fuzzy rules is performed by the fourth layer; and at last, by the summation of the fourth layer's outputs, the fuzzy system's output is computed via the fifth layer. Figure 2 showcases the MANFIS's structure, and in it, the ϕ_i , along with ϕ_{i+1} determines fuzzy sets.

In the first layer, the inputs are transformed into a linguistic type utilizing MF, which is expressed as:

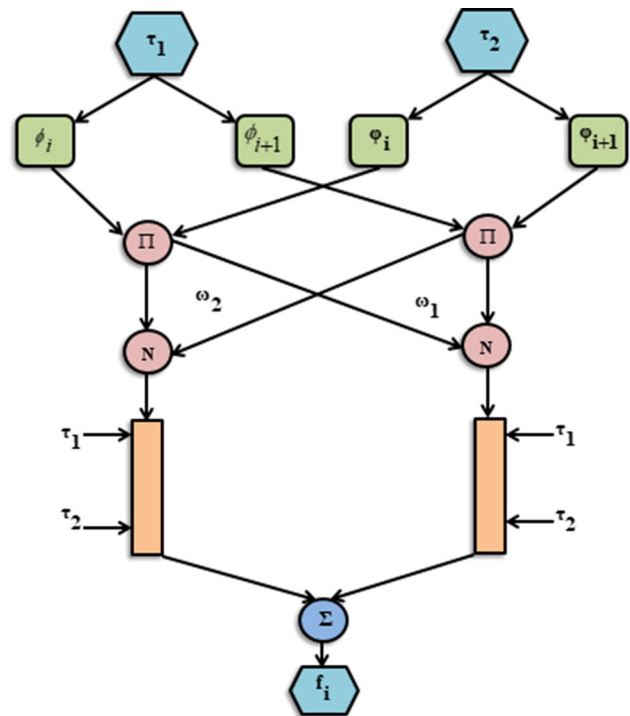


Fig. 2 Structure of the MANFIS

$$L_1 = \eta_{P_i}(\tau_1) \tag{1}$$

$$L_1 = \eta_{Q_i}(\tau_2) \tag{2}$$

wherein L_1 implies the first layer's output, η_{P_i} and η_{Q_i} signifies the membership value of 'η' MF which determines degree to which the given input satisfies the quantifier. Here, the triangular MF is regarded, and also, the range interval is fixed. The η is derived as follows:

$$\eta = \begin{cases} 0 & \tau_i \leq w \\ \frac{\tau_i - w}{m_m - \tau_i} & w < \tau_i \leq m_m \\ \frac{y - \tau_i}{y - m_m} & m_m < \tau_i < y \\ 0 & \tau_i \geq y \end{cases} \tag{3}$$

wherein w and y implies the lower as well as upper limit, τ_i signifies the inputted metrics $i = 1, 2$ together with m_m specifies the range values. Computing each node’s output in the second layer (Firing Strength (FS) of a rule) is the subsequent process in ANFIS, which is done by Eq. (4):

$$L_2 = \eta_{P_i}(\tau_1) \times \eta_{P_i}(\tau_2) \tag{4}$$

wherein L_2 implies the second layer’s output. Subsequently, the third layer normalizes the rule’s FS, and it is mathematically written as Eq. (5):

$$L_3 = \bar{\omega}_i = \frac{\omega_i}{\sum_{i=1}^n \omega_i} \tag{5}$$

wherein L_3 signifies the third layer’s output, $\bar{\omega}_i$ implies the normalized FS of i th rule together with ω_i signifies the rules’ FS which is the product of all input signals. In the fourth layer, the adaptive nodes gauge the output relying on L_3 as:

$$L_4 = \bar{\omega}_i r_i = \bar{\omega}_i (\alpha_i D_i + \beta_i D_{i+1} + \gamma_i) \tag{6}$$

wherein L_4 signifies the fourth layer’s output, r_i implies the IF–THEN rules, α_i , β_i , and γ_i ascertain the resultant parameter of the ‘ i th’ node. Lastly, the output is attained in the fifth layer, which is derived as:

$$L_5 = f_i = \sum_{i=1}^n \bar{\omega}_i r_i \tag{7}$$

wherein L_5 signifies the output layer and f_i implies the output. This last layer implies that whether the designed truncated code has deviated or not. If the deviation is present, the optimal inputted parameters are selected via the successive section.

3.3 Optimal Parameter Selection using ESSA

Here, the ESSA selects the optimal input parameters say tool path, tool diameter, sheet thickness, tool shape, wall angle, step size, together with spindle speed. Squirrel Search Algorithms (SSA) (Jain et al. 2017) commences with an arbitrary initial location of flying squirrels (δ) close to other populace-centred algorithms. Here, the input parameters are considered as squirrels. The δ ’s location is signified by means of a vector, on d dimensional search space. Thus, the δ can slide in 1D, 2D, 3D, or hyper-

dimensional search space as well as modify their location vectors.

3.3.1 Random initialization

There are n flying squirrels (δ) within a forest. In addition, those δ are taken as the input parameters. The i th flying squirrel’s location on the i th tree is signified via a vector,

$$\delta_i = (\delta_{i1}, \delta_{i2}, \delta_{i3}, \dots, \delta_{im}), \quad i = 1, 2, 3, \dots, n \tag{8}$$

wherein δ_{ij} signifies the j^{th} dimension of the i th flying squirrel together with m implies the number of dimensions. A uniform distribution is used to allocate the initial location of each flying squirrel in the forest which is given as follows

$$\delta_i = \delta_{\downarrow} + \zeta(0, 1) \times (\delta_{\uparrow} - \delta_{\downarrow}) \tag{9}$$

wherein δ_{\downarrow} and δ_{\uparrow} implied lower as well as upper bounds in j^{th} dimension of i th flying squirrel, correspondingly, and $\gamma(0, 1)$ signifies a uniformly distributed arbitrary number in the gamut $[0, 1]$.

After that, the FF value $v = (v_1, v_2, v_3, \dots, v_{ps})$ ’ of an individual δ ’s location is computed. The FF is derived as:

$$v_i = \min(\tau_1, \tau_2) \tag{10}$$

wherein ps signifies the number of populace size, and v_i signifies the FF. Subsequent to calculating the FF value, the fitness values of position for every δ is sorted out in ascending order. The δ on the Hickory Tree (HT) stated that it had the least fitness. The Acorn Tree (AT) is regarded as the subsequent r best δ ; from which also, they were deliberated to be moving in the direction of the HT. The remaining δ should be on the normal trees, some of which are also regarded to be moving on the way to the HT by means of arbitrary selection subsequent to meeting their everyday energy requirements, and also the remaining δ will move in the direction of the AT to satisfy their everyday energy requirements.

3.3.2 Generate new locations

For selecting the locations, ‘3’ scenarios are followed,

Scenario 1: The δ on the AT might move in the directions of the HT. The δ ’s new location can well be updated as:

$$\delta_{ct}^{t+1} = \begin{cases} \delta_{ct}^t + g_d \cdot S_c \cdot (\delta_{kt}^t - \delta_{ot}^t) & \text{if, } rand_1 \geq Pb \\ R_l & \text{otherwise} \end{cases} \tag{11}$$

wherein δ_{ct}^t and δ_{ct}^{t+1} signifies the flying squirrel’s location on the AT at t and $t + 1$ iteration, g_d indicates the gliding distance, S_c signifies the sliding constant, δ_{kt} implies the

flying squirrel on the HT, δ_{ot}^t implies the δ on a normal tree, $rand_1$ signifies the random number in the gamut of [0, 1], Pb implies the predator presence probabilities together with R_l signifies the random location.

Scenario 2: Some δ on the normal tree might move in the directions of AT to fulfill their everyday energy requirements. The new location of δ can well be updated as:

$$\delta_{ot}^{t+1} = \begin{cases} \delta_{ot}^t + g_d \cdot S_c \cdot (\delta_{ct}^t - \delta_{ot}^t) & \text{if, } rand_2 \geq Pb \\ R_l & \text{otherwise} \end{cases} \quad (12)$$

wherein δ_{ot}^{t+1} signifies the flying squirrel's location on the normal tree at t and $t + 1$ iteration, and $rand_2$ implies the random number 2 that is exhibited in the gamut [0, 1].

Scenario 3: Some δ that are on the normal trees, which have satisfied their everyday energy requirement, might go to HT for storing hickory nuts that can well be consumed during food shortages. Their new locations can well be attained as follows:

$$\delta_{ot}^{t+1} = \begin{cases} \delta_{ot}^t + g_d \cdot S_c \cdot (\delta_{kt}^t - \delta_{ot}^t) & \text{if, } rand_3 \geq Pb \\ R_l & \text{otherwise} \end{cases} \quad (13)$$

wherein $rand_3$ signifies the random number 3 exhibited in the gamut [0, 1].

3.3.3 Seasonal Monitoring

This step is done on SSA to escape as of local optimum solutions, which is exhibited in the subsequent steps:

In the first steps, the seasonal constant W_c is computed as:

$$W_c^t = \sqrt{\sum_{j=1}^m (\delta_{ct,j}^t - \delta_{kt,j}^t)^2} \quad (14)$$

wherein W_c^t signifies the seasonal constant at iteration t , $\delta_{kt,j}^t$ along with $\delta_{ct,j}^t$ implies the squirrel on the HT as well as AT at j^{th} dimension and m implies the total dimension.

Subsequently, in the second step, seasonal monitoring condition is verified via $W_c^t < W_{min}$ wherein W_{min} stands as the minimal value of seasonal constant calculated as follows:

$$W_{min} = \frac{10 e^{-6}}{(365)^{t/(t_{max}/2.5)}} \quad (15)$$

wherein t_{max} signifies the maximal number of iteration. The winter season is over if the specified condition is true, and again for food searching, the flying squirrels that lose their

abilities to probe the forest will arbitrarily relocate their searching positions.

$$\delta_{ot}^{t+1} = \delta_{\downarrow} + l_y \times (\delta_{\uparrow} - \delta_{\downarrow}) \quad (16)$$

wherein l_y implies the Cauchy distribution function. The levy distribution function is engaged in the normal SSA, which is not well fitting for the mechanical parameters, and it also has the over selection issue. Thus, here, the Cauchy distribution is employed, which is derived as:

$$l_y = \frac{1}{\pi} \frac{h_w}{(x_a - s_m) + h_w} \quad (17)$$

wherein s_m signifies the statistical mean, x_a implies the axis direction, and h_w signifies the half-width at half maximum.

3.3.4 Stopping criteria

If the maximal number of iterations is fulfilled, then the algorithm winds up. If not, generating new locations and checking seasonal monitoring conditions should be re-done.

Figure 3 illustrates the proposed ESSA's pseudo-code. Here, the squirrel is regarded as the inputted parameter. The squirrel's new locations are generated grounded on the '3' scenario, which is changed by means of the arbitrary number along with predator presence probability. The SPIF is designed by this ESSA.

4 Result and discussion

The performance assessment of the proposed geometric deviation prediction and optimal parameter selection approach in the SPIF metal forming method is exhibited. In the functioning platform of MATLAB, the proposed work is employed. The inputted and outputted values of the previously modelled truncated cone are regarded as the dataset. 80% of data is wielded for the intention of training as well as 20% is tested. Figure 4 showcases the structure of CAD/CAM simulation together with real-time manufactured truncated cone.

4.1 Performance analysis for geometric deviation prediction

Grounded on the accuracy, recall, precision, along with F-Measure, the analogy of the MANFIS's performance with the prevailing ANFIS, ANN, convolutional neural network (CNN) along with support vectors regressions (SVR) is performed here. Hence, centred on false positives, false negatives, true positives together with true negative metrics, the computation of metrics are performed. Table 1

Input: Input parameters, $\delta_i = (\delta_{i1}, \delta_{i2}, \delta_{i3}, \dots, \delta_{im})$
Output: Optimal parameters

Begin

Initialize input parameters $\delta_i = (\delta_{i1}, \delta_{i2}, \delta_{i3}, \dots, \delta_{im})$, roundness deviation τ_1 , position deviation τ_2 , seasonal constant W_c , and maximum iteration M_{it} .

Define initial location of each flying squirrel by, $\delta_i = \delta_{\downarrow} + \xi(0,1) \times (\delta_{\uparrow} - \delta_{\downarrow})$

Calculate fitness function, $v_i = \min(\tau_1, \tau_2)$

Set iteration $k_t = 1$

While ($k_t \leq M_{it}$) **do**

Generate new locations using 3 scenarios

// Scenario 1:

if ($rand_1 \geq Pb$) {

update the squirrel location $\delta_{ct}^{t+1} = \delta_{ct}^t + g_d \cdot S_c \cdot (\delta_{kt}^t - \delta_{ot}^t)$

} **else** {

$\delta_{ct}^{t+1} = R_t$

}

end if

// Scenario 2:

if ($rand_2 \geq Pb$) {

update the squirrel location $\delta_{ot}^{t+1} = \delta_{ot}^t + g_d \cdot S_c \cdot (\delta_{ct}^t - \delta_{ot}^t)$

} **else** {

$\delta_{ot}^{t+1} = R_t$

}

end if

// Scenario 3:

if ($rand_3 \geq Pb$) {

update the squirrel location $\delta_{ot}^{t+1} = \delta_{ot}^t + g_d \cdot S_c \cdot (\delta_{kt}^t - \delta_{ot}^t)$

} **else** {

$\delta_{ot}^{t+1} = R_t$

}

end if

Perform seasonal monitoring by using seasonal constant

Calculate fitness function

Set $k_t = k_t + 1$

End while

Return optimal parameters

End

Fig. 3 Pseudo-code for the ESSA

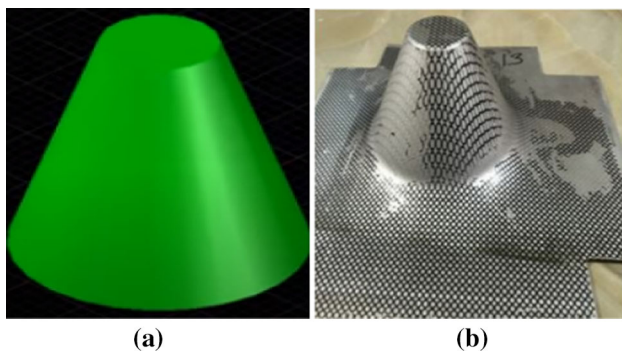


Fig. 4 Structure **a** CAD/CAM, and **b** manufactured truncated cone

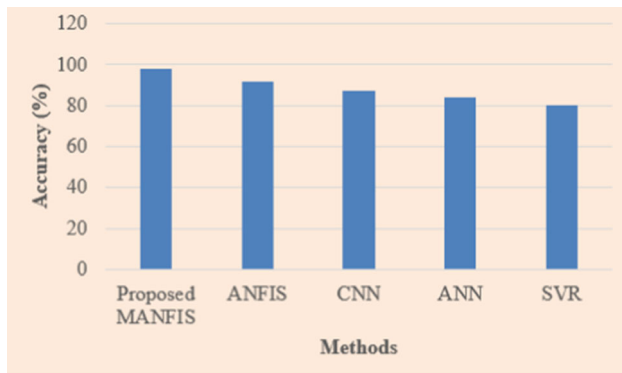
demonstrates the performance assessment of the disparate methods.

The MANFIS's performance evaluation with the prevailing ANFIS, CNN, ANN, along with SVR with reference to the '4' metrics is demonstrated in Table 1. The SPIF's geometric deviation in aluminium material is 97.90% precisely predicted by the proposed prediction technique. Centred on all the four metrics, the prevailing SVR comprise the bad result in Table 1. Next, the ANN is somewhat better when weighed against the SVR; however, compared to CNN and ANFIS, it has poor results. Finally, the prevailing methods are defeated by the MANFIS deviation prediction method. Therefore, it is finalized that more than the '4' prevailing techniques, the proposed MANFIS attains a greater rate of prediction.

The proposed MANFIS's accuracy with the prevailing four methods is depicted in Fig. 5. In present days, for the

Table 1 Performance analysis of the proposed MANFIS with the existing ANFIS, ANN, CNN, and SVR-based on statistical metrics

Methods	Accuracy (%)	Precision (%)	Recall (%)	F-Measure (%)
Proposed MANFIS	97.90	96.78	95.84	96.23
ANFIS	91.56	90.23	89	90.21
CNN	87.34	88.23	87.45	88.24
ANN	84.23	85.23	85.34	85.24
SVR	79.90	80	81.23	80.89

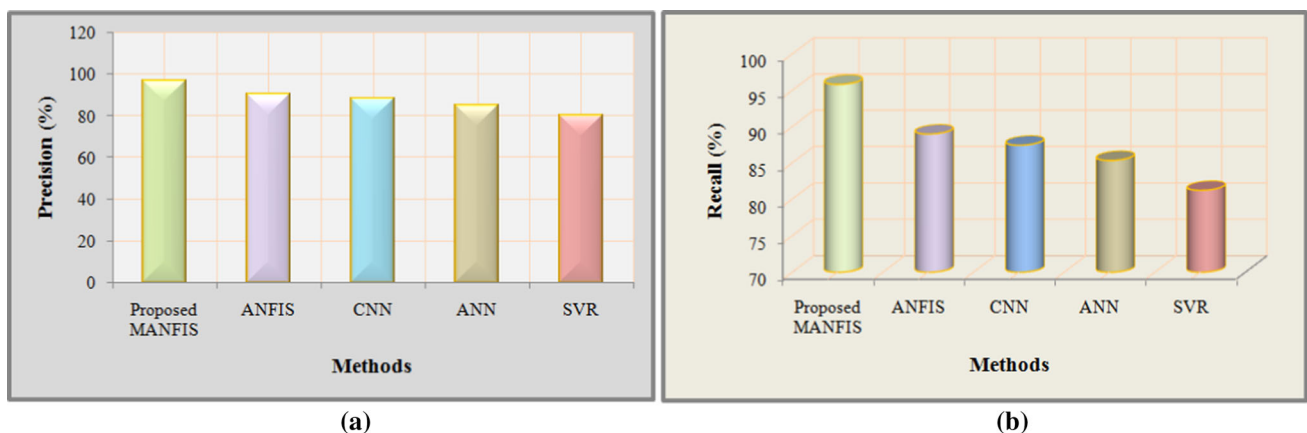
**Fig. 5** Comparative analysis of the proposed and existing deviation prediction methods based on accuracy metric

geometric deviation prediction, machine learning algorithms are utilized. However, each comprises a problem because of which the prediction's accuracy is worse. Grounded on the output, more adjustments are taken, if the prediction's output is correct. Thus, the prediction's accuracy is a significant measure. For the existing ANFIS, CNN, ANN together with SVR techniques, the obtained accuracy are 91.56%, 87.34%, 84.23%, and 79.90%, respectively, nevertheless, the proposed MANFIS's attained accuracy is 97.90%. Thus, Fig. 5 demonstrates that the proposed MANFIS achieves greater prediction accuracy than that of the existent techniques.

The graphical depiction of the MANFIS's comparative evaluation with the prevailing four techniques concerning

(a) precision along with (b) recall metrics is showcased in Fig. 6. Precision stands as the gauge of quality and recall stands as a gauge of quantity. More pertinent results are rendered by the method if the prediction technique comprises a greater precision value, and most of the pertinent results are returned by the method if the recall is greater. The MANFIS comprises the precision of 96.78%, which is larger than the prevailing ANFIS, CNN, ANN, and SVR (i.e.) 90.23%, 88.23%, 85.23%, and 80%, respectively. Likewise, centred on the recall metric, the attained recall value of the proposed framework is 95.84%, which outweighs the recall attained by the prevailing techniques. Lastly, as of Fig. 6, it is illustrated that the MANFIS comprises good results than the prevailing method.

The proposed MANFIS's performance is analysed with the prevailing ANFIS, CNN, ANN, along with SVR relating to F-measure metrics in Fig. 7. The F-measure stands as the gauge of the test's accuracy and the F-measure's outcome are acquired by combining the recall with precision metrics. Previously, centred on the precision together with recall metrics, the attained results of the proposed MANFIS outweighs the prevailing techniques such that grounded upon the F-measure metric as well, the greatest F-measure value attained by means of the proposal is 96.23%. The ANFIS is a lot better than every other metrics, and its result is 90.21%. Whilst the SVR alone encompasses bad results (i.e.) 80.89% and CNN together with ANN methods comprise a bad outcome of 88.24% as

**Fig. 6** Graphical representation for the comparative analysis of the proposed and existing methods in terms of a precision, and b recall

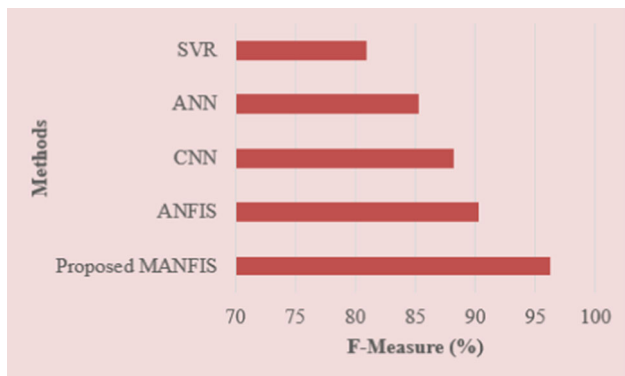


Fig. 7 F-Measure analysis for the proposed and existing methods

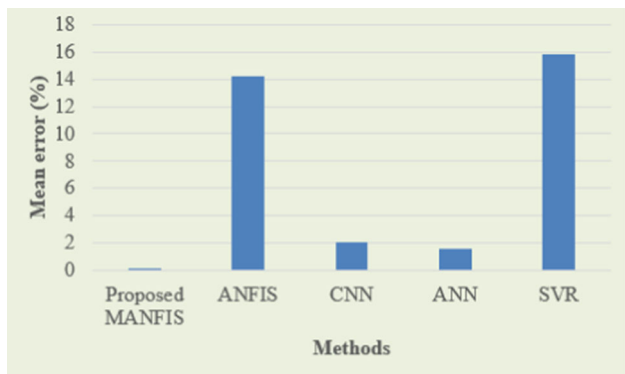


Fig. 8 Mean error analysis for the proposed and existing methods

well as 85.25%, respectively. Hence, the discussion validates that the MANFIS comprises the superior result.

Figure 8 analyses the performance of the proposed MANFIS with the existing ANFIS, CNN, ANN, and SVR with respect to mean error. The proposed MANFIS attained mean error of 0.017% whilst other methods showed the mean error percentage higher than the proposed method. This means that proposed method showed superior performance in terms of mean error.

Figure 9 analyses the performance of the proposed MANFIS with the existing deep belief network (DBN)

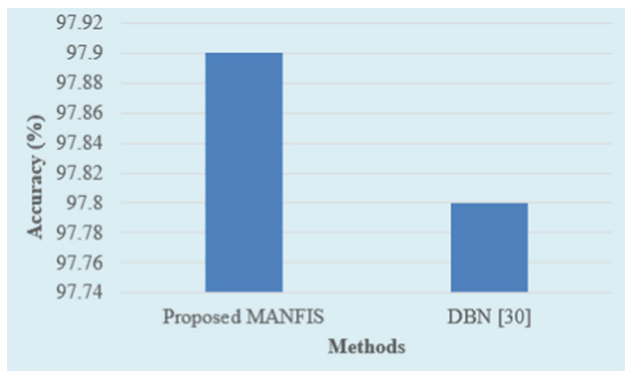


Fig. 9 Accuracy analysis

(Akrichi and Abbassi 2019) with respect to accuracy. The proposed MANFIS attained the accuracy level of 97.90% whilst the DBN acquired the accuracy level of 97.8%. This shows that the proposed method performs well in finding geometric deviation than other considered method.

4.2 Performance analysis for optimal parameter selection

The performance analogy of the optimal parameters selection techniques is performed in this section. Without employing optimization, it is analogized with the proposed ESSA-centred optimal parameter selection together with the existent optimal parameter selection techniques, like GA, SSA, along with particle swarms optimization (PSO) concerning the roundness deviation and position deviation. Therefore, the geometric deviations are gauged by means of computing the mean square error (MSE) betwixt the actual output and the attained output of the designed truncated cone shape.

The roundness deviation’s analysis without and with-selection of optimal parameter utilizing proposed ESSA with prevailing SSA, PSO, and GA centred on MSE is showcased in Fig. 10. An imperative geometric metric is roundness. The geometric accuracy is bad if the roundness greatly deviates. Hence, the deviation measurement is done by error. The shape manufactured with optimal parameters selection comprises low error than that manufactured without-selection of optimal parameters that encompass 15.34 errors. The selection performed in the with-optimal parameter selection by proposed ESSA merely comprises 2.4 errors. There is the least error in the with-selection of the optimal parameter. Greater error is encompassed by the existent PSO and GA. Therefore, utilizing the proposed ESSA, the optimal parameter selection delivers values that are nearer to the actual output than the other techniques.

The optimal parameter selection’s performance by utilizing the proposed ESSA, SSA, PSO, and GA with and without-selection of the optimal parameter in relation to the

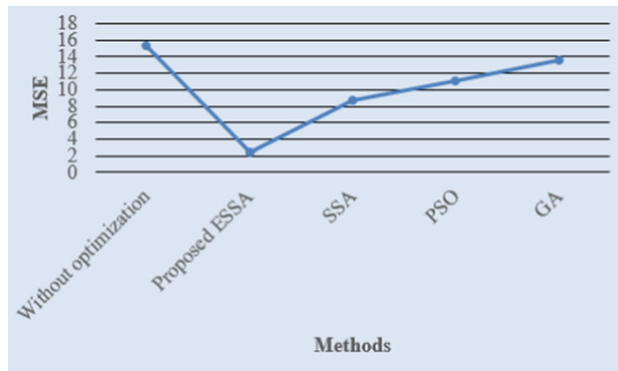


Fig. 10 Analysis of the roundness deviation based on MSE



Fig. 11 Analysis of the position deviation based on MSE

position deviation concerning the MSE metric is analysed in Fig. 11. Selection of optimal parameter by utilizing ESSA contains 3.2 error of position deviation, SSA encompasses 8.02 errors, PSO comprises 10.09 errors together with GA contains 12.88 errors. The position deviation manufacturer errors of 15.12 are contained by the without optimal parameters selection. Hence, this explains that the position deviation encompassed by the with-optimal parameters selection is lesser than that contained by the without-selection of the optimal parameter. In the selection of optimal parameter, the proposed ESSA comprise good result than the prevailing techniques.

Centred on the number of iterations, the fitness value of the proposed ESSA, SSA, PSO, and GA algorithm is scrutinized in Fig. 12. The algorithm is signified as an effective algorithm for selecting the optimal parameters if it contains the best fitness value. The fitness values are incremented as the iteration level is incremented. In all iteration, the proposed ESSA consists of the largest fitness value as the GA's fitness value is the least and the SSA along with PSO contains the fitness value in the middle. Lastly, it exhibits that the ESSA has a better outcome than the prevailing algorithms.

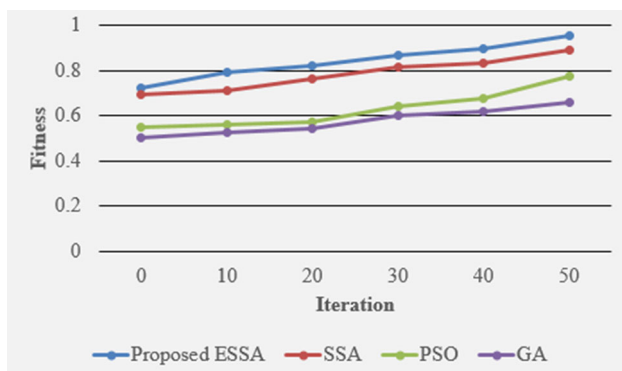


Fig. 12 Fitness versus Iteration

5 Conclusion

An improved flexible manufacturing process that forms the clamped sheet into the intended shape by a hemispherical tool's movement is called the SPIF process. However, it contains a geometric deviation problem. Therefore, for solving that problem, initially, the prediction of geometric deviation is performed grounded on the proposed MANFIS, and next, the selection of optimal parameters is done by employing the ESSA, and for additional manufacturing, the optimal parameters are recommended to the SPIF model. In the designing of SPIF, the CAD/CAM software is employed for designing the chosen shapes and CMM is employed for gauging the geometric metrics. By utilizing the earlier manufactured shape's inputted and outputted values, which is regarded as the dataset, the analysis of the system's performance is performed. The performance evaluation is performed in 2 segments, namely examining the geometric deviation's performance and performance analysis of the optimal parameter selection. The proposed MANFIS's performance is analogized with the prevailing ANFIS, CNN, ANN, together with SVR with respect to the accuracy, precision, recall, along with F-measure, in the geometrics deviation prediction analysis. The proposed ESSA's performance is analogized with the prevailing SSA, PSO, along with GA, in the optimal parameter selection analysis part and is also analogized with the without-optimal parameter selection grounded on MSE. A better result is attained by the proposed methods when contrasted to the existent methods by obtaining values of 97.90%, 96.78%, 95.84%, 96.23%, and 0.017% for accuracy, precision, recall, F-measure along with mean error. 2.4 roundness deviation and 3.2 position deviation are possessed by the proposed ESSA-centred manufacturing. This is because of the alterations performed in the methods incorporated in the proposed work namely the triangular membership function in MANFIS. From the entire analysis, it is viewed that the attained results of the proposed techniques are high than the prevailing techniques. In the future, by utilizing improved algorithms, the system can well be protracted, and for fitness function, more metrics can well be considered, so as to greatly decrease the GE.

Declarations

Conflict of interest The author has no conflict of interest.

References

Akrichi S, Abbassi A, Abid S, Ben Yahia N (2019) Roundness and positioning deviation prediction in single point incremental

- forming using deep learning approaches. *Adv Mech Eng* 11(7):1–15
- Ali RA, Chen W, Al-Furjan MSH, Jin X, Wang Z (2019) Experimental investigation and optimal prediction of maximum forming angle and surface roughness of an AL/SUS bimetal sheet in an incremental forming process using machine learning. *Materials* 12(24):1–20
- Alinaghian M, Alinaghian I, Honarpisheh M (2019) Residual stress measurement of single point incremental formed Al/Cu bimetal using incremental hole-drilling method. *Int J Lightweight Mater Manuf* 2(2):131–139
- Amino M, Mizoguchi M, Terauchi Y, Maki T (2014) Current status of “dieless” Amino’s incremental forming. *Procedia Eng* 81:54–62. <https://doi.org/10.1016/j.proeng.2014.09.128>
- Azevedo NG, Farias JS, Bastos RP, Teixeira P, Davim JP, Alves de Sousa RJ (2015) Lubrication aspects during Single Point Incremental Forming for steel and aluminum materials. *Int J Precis Eng Manuf* 16(3):589–595. <https://doi.org/10.1007/s12541-015-0079-0>
- Cao J, Xia ZC, Gutowski TG and Roth J (2012) A hybrid forming system: electrical-assisted double side incremental forming (EADSIF) process for enhanced formability and geometrical flexibility, Northwestern University, Document ID: DE-EE0003460
- Dabwan A, Ragab AE, Saleh MA, Anwar S, Ghaleb AM, Rehman AU (2020) Study of the effect of process parameters on surface profile accuracy in single-point incremental sheet forming of AA1050-H14 aluminum alloy. *Adv Mater Sci Eng*. <https://doi.org/10.1155/2020/7265941>
- Dai P, Chang Z, Li M, Chen J (2019) Reduction of geometric deviation by multi-pass incremental forming combined with tool path compensation for non-axisymmetric aluminum alloy component with stepped feature. *Int J Adv Manuf Technol* 102:809–817. <https://doi.org/10.1007/s00170-018-3194-0>
- Fischer JD, Woodside MR, Gonzalez MM, Lutes NA, Bristow DA, Landers RG (2019) Iterative learning control of single point incremental sheet forming process using digital image correlation”. *Procedia Manuf* 34:940–949. <https://doi.org/10.1016/j.promfg.2019.06.108>
- Fu Z, Mo J, Han F, Gong P (2012) Tool path correction algorithm for single-point incremental forming of sheet metal. *Int J Adv Manuf Technol* 64(9–12):1239–1248
- Hartmann C, Opritescu D, Volk W (2016) An artificial neural network approach for tool path generation in incremental sheet metal free-forming. *J Intell Manuf* 30:757–770. <https://doi.org/10.1007/s10845-016-1279-x>
- Ibrahim AK, Hamdan WK (2015) Application of adaptive neuro-fuzzy inference system for prediction of surface roughness in incremental sheet metal forming process. *Eng Technol J* 33:380–399
- Isidore BBL, Hussain G, Shamchi SP, Khan WA (2016) Prediction and control of pillow defect in single point incremental forming using numerical simulations. *J Mech Sci Technol* 30(5):2151–2161. <https://doi.org/10.1007/s12206-016-0422-0>
- Jain M, Singh V, Rani A (2017) A novel nature-inspired algorithm for optimization squirrel search algorithm. *Swarm Evol Comput*. <https://doi.org/10.1016/j.swevo.2018.02.013>
- Khan MS, Coenen F, Dixon C, El-Salhi S, Penalva M, Rivero A (2014) An intelligent process model: predicting springback in single point incremental forming. *Int J Adv Manuf Technol* 76(9–12):2071–2082. <https://doi.org/10.1007/s00170-014-6431-1>
- Kumar N, Belokar RM (2019) Experimental investigation of geometric accuracy in single point incremental forming process of an aluminium alloy. *Int J Mater Eng Innov* 10(1):46–59. <https://doi.org/10.1504/ijmatei.2019.097914>
- Li R-J, Li M-Z, Qiu N-J, Cai Z-Y (2014) Surface flexible rolling for three-dimensional sheet metal parts. *J Mater Process Technol* 214(2):380–389. <https://doi.org/10.1016/j.jmatprotec.2013.09.008>
- Li Y, Daniel WJT, Liu Z, Lu H, Meehan PA (2015a) Deformation mechanics and efficient force prediction in single point incremental forming. *J Mater Process Technol* 221:100–111. <https://doi.org/10.1016/j.jmatprotec.2015.02.009>
- Li Y, Lu H, Daniel WJT, Meehan PA (2015b) Investigation and optimization of deformation energy and geometric accuracy in the incremental sheet forming process using response surface methodology. *Int J Adv Manuf Technol* 79(9–12):2041–2055. <https://doi.org/10.1007/s00170-015-6986-5>
- Liu Z, Li Y (2019) Small data-driven modeling of forming force in single point incremental forming using neural networks. *Eng Comput*. <https://doi.org/10.1007/s00366-019-00781-6>
- Lu H, Kearney M, Li Y, Liu S, Daniel WJT, Meehan PA (2015) Model predictive control of incremental sheet forming for geometric accuracy improvement. *Int J Adv Manuf Technol* 82(9–12):1781–1794. <https://doi.org/10.1007/s00170-015-7431-5>
- Maji K, Kumar G (2019) Inverse analysis and multi-objective optimization of single-point incremental forming of AA5083 aluminum alloy sheet. *Soft Comput* 24:4505–4521. <https://doi.org/10.1007/s00500-019-04211-z>
- Mohammadi A, Vanhove H, Van Bael A, Duflou JR (2014) Towards accuracy improvement in single point incremental forming of shallow parts formed under laser assisted conditions. *Int J Mater Form* 9(3):339–351. <https://doi.org/10.1007/s12289-014-1203-x>
- Mulay A, Ben BS, Ismail S, Kocanda A (2019) Prediction of average surface roughness and formability in single point incremental forming using artificial neural network. *Arch Civil Mech Eng* 19(4):1135–1149. <https://doi.org/10.1016/j.acme.2019.06.004>
- Panjwani D, Priyadarshi S, Jain PK, Samal MK, Roy JJ, Roy D, Tandon P (2017) A novel approach based on flexible supports for forming non-axisymmetric parts in SPISF. *Int J Adv Manuf Technol* 92(5–8):2463–2477. <https://doi.org/10.1007/s00170-017-0223-3>
- Said LB, Mars J, Wali M, Dammak F (2017) Numerical prediction of the ductile damage in single point incremental forming process. *Int J Mech Sci* 131–132:546–558. <https://doi.org/10.1016/j.jimecs.2017.08.026>
- Sbayti M, Bahloul R, BelHadjsalah H, Zemzemi F (2017) Optimization techniques applied to single point incremental forming process for biomedical application. *Int J Adv Manuf Technol* 95(5–8):1789–1804. <https://doi.org/10.1007/s00170-017-1305-y>
- Sbayti M, Bahloul R, Belhadjsalah H (2019) Efficiency of optimization algorithms on the adjustment of process parameters for geometric accuracy enhancement of denture plate in single point incremental sheet forming. *Neural Comput Appl* 32:8829–8846. <https://doi.org/10.1007/s00521-019-04354-y>
- Taherkhani A, Basti A, Nariman-Zadeh N, Jamali A (2018) Achieving maximum dimensional accuracy and surface quality at the shortest possible time in single-point incremental forming via multi-objective optimization. *Proc Inst Mech Eng Part B J Eng Manuf* 233(3):900–913. <https://doi.org/10.1177/0954405418755822>
- Zhang Z, Zhang H, Shi Y, Moser N, Ren H, Ehmann KF, Cao J (2016) Springback reduction by annealing for incremental sheet forming”. *Procedia Manuf* 5:696–706. <https://doi.org/10.1016/j.promfg.2016.08.057>

Publisher's Note Springer Nature remains neutral with regard to jurisdictional claims in published maps and institutional affiliations.